HHS Public Access

Author manuscript

J Thorac Oncol. Author manuscript; available in PMC 2021 August 13.

Published in final edited form as:

J Thorac Oncol. 2020 October ; 15(10): 1599–1610. doi:10.1016/j.jtho.2020.06.001.

A Grading System for Invasive Pulmonary Adenocarcinoma: A Proposal From the International Association for the Study of Lung Cancer Pathology Committee

Andre L. Moreira, MD, PhD[a,*], **Paolo S. S. Ocampo, MD, PhD**[a], **Yuhe Xia**[b], **Hua Zhong**[b], **Prudence A. Russell, MD**[c], **Yuko Minami, MD, PhD**[d], **Wendy A. Cooper, MD**[e], **Akihiko Yoshida, MD, PhD**[f], **Lukas Bubendorf, MD**[g], **Mauro Papotti, MD**[h], **Giuseppe Pelosi, MD**[i,j], **Fernando Lopez-Rios, MD, PhD, FIAC**[k], **Keiko Kunitoki, MD**[l], **Dana Ferrari-Light, DO**[m], **Lynette M. Sholl, MD**[n], **Mary Beth Beasley, MD**[o], **Alain Borczuk, MD**[p], **Johan Botling, MD, PhD**[q], **Elisabeth Brambilla, MD, PhD**[r], **Gang Chen, MD**[s], **Teh-Ying Chou, MD, PhD**[t], **Jin-Haeng Chung, MD, PhD**[u], **Sanja Dacic, MD, PhD**[v], **Deepali Jain, MD**[w], **Fred R. Hirsch, MD, PhD**[x], **David Hwang, MD, PhD**[y], **Sylvie Lantuejoul, MD, PhD**[z], **Dongmei Lin, MD**[aa], **John W. Longshore, PhD**[bb], **Noriko Motoi, MD, PhD**[f], **Masayuki Noguchi, MD**[cc], **Claudia Poleri, MD**[dd], **Natasha Rekhtman, MD, PhD**[ee], **Ming-Sound Tsao, MD**[ff], **Erik Thunnissen, MD, PhD**[gg], **William D. Travis, MD**[ee], **Yasushi Yatabe, MD, PhD**[f], **Anja C. Roden, MD**[hh], **Jillian B. Daigneault, PhD**[ii], **Ignacio I. Wistuba, MD**[jj], **Keith M. Kerr, MD**[kk], **Harvey Pass, MD**[m], **Andrew G. Nicholson, MD**[ll,mm], **Mari Mino-Kenudson, MD**[nn]

[a]Department of Pathology, New York University Langone Health, New York, New York [b]Department of Biostatistics, New York University Langone Health, New York, New York [c]Department of Pathology, St. Vincent's Hospital, Victoria, Australia [d]Department of Pathology, Ibarakihigashi National Hospital, Tokai, Japan [e]Department of Pathology, Royal Prince Alfred Hospital, Camperdown, Australia [f]Department of Diagnostic Pathology, National Cancer Center Hospital, Tokyo, Japan [g]Institute of Medical Genetics and Pathology, University Hospital Basel, University of Basel, Switzerland [h]Department of Oncology, University of Turin, Turin, Italy [i]Department of Pathology, University of Milan, Milan Italy [j]IRCCS MultiMedica, Milan Italy [k]Pathology-Laboratorio de Dianas Terapeuticas, HM Hospitales, Madrid, Spain [l]Harvard T.H. Chan School of Public Health, Boston, Massachusetts [m]Department of Surgery, New York University Langone Health, New York, New York [n]Department of Pathology, Brigham and Women's Hospital, Harvard Medical School, Boston, Massachusetts [o]Department of Pathology, Icahn School of Medicine, Mount Sinai Health System, New York, New York [p]Department of Pathology, Weill Cornell Medicine, New York, New York [q]Department of Immunology, Genetics and Pathology, Rudbeck Laboratory, Uppsala University Hospital, Uppsala, Sweden [r]Department of Anatomic Pathology and Cytology, Université Grenoble Alpes, Grenoble, France [s]Department fo Pathology, Zhongshan Hospital, Fudan University, Shanghai, People's Republic of China

[*]Address for correspondence: Andre L. Moreira, MD, PhD, Department of Pathology, New York University Langone Health, 560 First Ave., TH 4-15B, New York, NY 10016. andre.moreira@nyumc.org.

Supplementary Data

Note: To access the supplementary material accompanying this article, visit the online version of the *Journal of Thoracic Oncology* at www.jto.org and at https://doi.org/10.1016/j.jtho.2020.06.001.

[t]Department of Pathology, Taipei Veterans General Hospital, Taipei, Taiwan [u]Department of Pathology, Seoul National University Bundang Hospital, Seoul, South Korea [v]Department of Pathology, University of Pittsburgh Medical Center, Pittsburgh, Pennsylvania [w]Department of Pathology, All India Institute of Medical Sciences, New Delhi, India [x]Center for Thoracic Oncology, The Tisch Cancer Institute, New York, New York [y]Department of Laboratory Medicine & Molecular Diagnostics, Sunnybrook Health Sciences Centre, Toronto, Ontario, Canada [z]Department fo Pathology, Centre Léon Bérard Unicancer, Lyon, France [aa] Department of Pathology, Peking University Cancer Hospital and Institute, Beijing, People's Republic of China [bb] Carolinas Pathology Group, Atrium Health, Charlotte, North Carolina [cc] Department of Pathology, University of Tsukuba, Tsukuba, Japan [dd] Office of Pathology Consultants, Buenos Aires, Argentina [ee] Department of Pathology, Memorial Sloan Kettering Cancer Center, New York, New York [ff] University Health Network, Princess Margaret Cancer Centre, Toronto, Ontario, Canada [gg] Department of Pathology, VU University Medical Center, Amsterdam, The Netherlands [hh] Department of Laboratory Medicine and Pathology, Mayo Clinic, Rochester, Minnesota [ii] International Association for the Study of Lung Cancer, Aurora, Colorado [jj] Department of Pathology, The University of Texas MD Anderson Cancer Center, Houston, Texas [kk] Department of Pathology, Aberdeen Royal Infirmary, Aberdeen, United Kingdom [ll] Department of Pathology, Royal Brompton and Harefield NHS Foundation Trust, London, United Kingdom [mm] National Heart and Lung Institute, Imperial College, London, United Kingdom [nn] Department of Pathology, Massachusetts General Hospital, Harvard Medical School, Boston, Massachusetts

Abstract

Introduction: A grading system for pulmonary adenocarcinoma has not been established. The International Association for the Study of Lung Cancer pathology panel evaluated a set of histologic criteria associated with prognosis aimed at establishing a grading system for invasive pulmonary adenocarcinoma.

Methods: A multi-institutional study involving multiple cohorts of invasive pulmonary adenocarcinomas was conducted. A cohort of 284 stage I pulmonary adenocarcinomas was used as a training set to identify histologic features associated with patient outcomes (recurrence-free survival [RFS] and overall survival [OS]). Receiver operating characteristic curve analysis was used to select the best model, which was validated (n = 212) and tested (n = 300, including stage I–III) in independent cohorts. Reproducibility of the model was assessed using kappa statistics.

Results: The best model (area under the receiver operating characteristic curve [AUC] = 0.749 for RFS and 0.787 for OS) was composed of a combination of predominant plus high-grade histologic pattern with a cutoff of 20% for the latter. The model consists of the following: grade 1, lepidic predominant tumor; grade 2, acinar or papillary predominant tumor, both with no or less than 20% of high-grade patterns; and grade 3, any tumor with 20% or more of high-grade patterns (solid, micropapillary, or complex gland). Similar results were seen in the validation (AUC = 0.732 for RFS and 0.787 for OS) and test cohorts (AUC = 0.690 for RFS and 0.743 for OS), confirming the predictive value of the model. Interobserver reproducibility revealed good agreement (k = 0.617).

Conclusions: A grading system based on the predominant and high-grade patterns is practical and prognostic for invasive pulmonary adenocarcinoma.

Keywords

Adenocarcinoma; Tumor grading; Lung; Model; Prognosis

Introduction

Tumor grading has been a traditional component of pathologic evaluation and offers guidance to therapy and patient management in many organ systems.[1–5] However, there is no consensus on a grading system for invasive pulmonary adenocarcinoma. The 2015 WHO classification of pulmonary adenocarcinoma,[6] based on the predominant histologic pattern, has consistently been found to correlate with prognosis and separates adenocarcinoma into the three following prognostic groups: low grade (lepidic predominant); intermediate grade (acinar or papillary predominant); and high grade (solid or micropapillary predominant). There are also suggestions that the classification and stratification by the predominant pattern is predictive of response to adjuvant chemotherapy.[7]

Pulmonary adenocarcinomas are histologically heterogeneous and present with multiple combinations of patterns and proportions. When classified by the predominant pattern only, the acinar subtype is the most prevalent (estimated at 40%–50% of patients) and carries the widest spectrum of prognoses.[8–12]

In addition to the five major histologic patterns, several other patterns have been recognized to occur in the lung and are also recognized in adenocarcinomas of other organs.[13] These include cribriform (defined as nests of neoplastic cells with sieve-like perforations) and fused gland (defined as poorly formed fused glands without intervening stroma or in a ribbon-like formation with irregular borders and single cells infiltrating desmoplastic stroma) patterns. The cribriform pattern in lung adenocarcinoma was recognized in the 2015 WHO classification, but it was decided not to create a new subtype but rather describe this pattern as a part of a high-grade pattern of the acinar subtype.[6]

These complex glandular patterns (high-grade acinar) have been found to be associated with high mitotic rate, tumor necrosis, and lymphovascular invasion in the lungs.[14,15] Furthermore, current evidence is in agreement that these complex glandular patterns carry poor prognosis similar to that of high-grade histologic types (solid and micropapillary).[11,14–19] Lack of appreciation of these patterns, however, may have led to uncertainty in tumor classification and poor reproducibility, because some investigators may have classified these patterns as intermediate grade (acinar) or high grade (solid). Thus, it is important to identify these “nontraditional patterns” and classify them as complex glands separately from conventional acinar pattern.

Recent studies have proposed the inclusion of a number of additional pathologic features, such as secondary histologic patterns,[20] nuclear grade,[21–23] mitotic grade,[22–24] presence of spread through airspaces (STAS),[25–29] and necrosis,[30,31] to the predominant pattern classification in an attempt to improve the grading scheme. All these additional histologic

features have been reported to have a prognostic value; however, most studies evaluated these features as a single parameter and did not take into account the heterogeneity of pulmonary adenocarcinomas. There has been no systematic approach to evaluate and incorporate multiple proposed prognostic factors into a grading system.

Supplementing the classification of pulmonary adenocarcinoma with a grading system will help define prognostic groups and provide a common path to prognostic stratification of patients with pulmonary adenocarcinoma who may benefit from the changing landscape of emerging management and treatment options.

The International Association for the Study of Lung Cancer (IASLC) pathology committee, therefore, has conducted a systematic study to evaluate a set of histologic features that have been described as prognostic indicators and establish a grading system for resected invasive pulmonary adenocarcinoma.

Material and Methods

Study Cohorts

A multi-institutional study involving multiple well-annotated cohorts of resected pulmonary adenocarcinoma was conducted. All cases were staged according to the eighth edition of American Joint Committee on Cancer staging manual[1] and had at least 5 years of follow-up. Four independent data sets were included in the study. Each data set collection had the approval of their respective Institution Review Board. The American data sets were collected following the Health Insurance Portability and Accountability Act regulations.

One cohort composed of 284 stage I cases (New York University Langone Health, New York, NY) was used as a training set for evaluation of the best parameters to be used in constructing a grading system. The findings were validated in a cohort of 212 stage I cases (Massachusetts General Hospital, Boston, MA), and the final model was tested in another data set of 300 stage I to III cases (Brigham and Women's Hospital, Boston, MA and St. Vincent's Hospital, Melbourne, Australia). Demographic information for all cohorts is illustrated in Table 1.

Histologic Evaluation

The cases in the training and validation cohorts were reviewed by the submitting pathologist (ALM, MMK) and evaluated for the histologic parameters described subsequently. The cases in the test cohort were not reviewed specifically for this study, as they represent historical sets from the provider's institution (LMS, PAR).

Comprehensive Histologic Subtyping.—This was performed in all the training and validation cohort cases using the semiquantitative estimation of all patterns of 5% increment as suggested by the current WHO classification of lung tumor.[6] All five patterns recognized by WHO and nontraditional patterns, such as cribriform and fused glands (complex glandular patterns), were included to a sum of 100%. Figure 1A–F illustrates examples of complex glandular patterns. Adenocarcinoma in situ, minimally invasive adenocarcinomas,

multifocal adenocarcinomas, invasive mucinous adenocarcinoma, and other variants of adenocarcinoma were excluded from the study.

Nuclear Grade.—This was determined, as previously described,[21–23] as follows: Grade 1: round, regular nuclei with evenly dispersed chromatin and without inconspicuous nucleoli, up to 2× to 3× the size of a lymphocyte. Grade 2: round, mildly irregular, minimally pleomorphic nuclei without inconspicuous nucleoli, up to 2× to 3× the size of a lymphocyte. Grade 3: pleomorphic nuclei with prominent nucleoli, greater than 5× the size of a lymphocyte (Supplementary Fig. 1).

Mitotic Grade.—This was determined, as previously described,[22,23] as follows: Grade 1: 0 to 1 mitotic figure/10 high-power field (hpf). Grade 2: 2 to 4 mitotic figures/10 hpf. Grade 3: greater than or equal to 5 mitotic figures/10 hpf.

Cytologic Grade.—This was defined as follows: low grade, low degree of cell pleomorphism and small cell size; high grade, high degree of cell pleomorphism and large cell size (Supplementary Fig. 1).

Hot-Spot Determination.—Given the heterogeneity of pulmonary adenocarcinomas, nuclear grade, mitotic grade, and cytologic grade were recorded at “hot-spot” (areas of highest grade), and the corresponding histologic pattern of the hot-spot was also recorded.

STAS.—It was defined as previously reported,[25] briefly, tumor cells either in micropapillary clusters or solid nests or single cells within airspaces beyond the edge of the main tumor. STAS was recorded as present or absent.

Necrosis.—Necrosis within the tumor was also recorded as present or absent.

Model Construction

Because the predominant pattern is used in the classification of adenocarcinoma and reveals a consistent stratification by prognostic groups, the predominant pattern was used as the basis for the model. In addition, several approaches were evaluated and compared with respect to how best they represent histologic features to achieve best prognostic discrimination. The histologic patterns were evaluated as follows: “weighted average” defined as the sum of the proportions of all patterns multiplied by their hazard ratios for recurrence derived from the coefficients of a Cox proportional model measuring the association between time to recurrence and predominant pattern; “binary pattern,” in which the histologic patterns were treated as present or absent independent of their proportions but assigned a number according to previously established grades (1: lepidic; 2: acinar, papillary; 3: solid, micropapillary, complex glands); and “numeric,” in which the numerical proportion of that pattern was taken into consideration.

Different studies have applied variable percentage cutoffs to define the amount of high-grade pattern required to predict unfavorable patient outcomes.[31–34] We, therefore, attempted to identify the percentage of high-grade pattern providing the best discriminatory performance. The Youden Index was used to select the best cutoff of the percentage of high-grade pattern

to achieve a positive prediction value greater than or equal to 85%. We used both recurrence and death as outcomes and compared the cutoffs for both.

Finally, the role of other histologic features (nuclear grade, mitotic grade, cytologic grade, STAS, and necrosis) were evaluated.

Statistical Analysis

Model Construction.—Descriptive statistics were presented as means with SDs for continuous variables and as frequencies with proportions for categorical variables. Continuous variables and categorical variables were compared between groups using two-sample *t* tests and chi-square test. Recurrence-free survival (RFS) and overall survival (OS) were calculated from the time of initial diagnosis to the time of first recurrence or death, respectively. The time of the last follow-up was used for censored patients. Cox proportional hazard regressions were used to predict recurrence status in the training cohort. The candidate predictors were histologic features and clinical characteristics that included age, sex, and pathologic stage. The model was selected by assessing each predictor's significance and minimizing Akaike's information criterion. A linear combination of the selected model predictors, weighted by regression coefficients, was defined as the risk score and applied to the cohort. We estimated prognostic discrimination ability by identifying the area under the receiver operating characteristic curve (AUC) values for recurrence and death, respectively. In addition, the concordance index (C-index), which is similar to AUC for binary outcomes, was used to indicate the discriminatory ability to predict RFS and OS, respectively. A value of 0.5 indicates that the model has no discriminatory ability, and a value of 1.0 indicates that the model has perfect discriminatory ability. A two-tailed *p* value less than 0.05 was used to establish statistical significance. All data were analyzed using R version 3.5.1.

Survival Analysis.—Survival curves were plotted using Kaplan-Meier curves, and differences between strata of grade in the proposed (IASLC) and predominant pattern-based grading systems for OS and RFS were determined using log-rank tests. Data were analyzed using R version 3.6.1. The *p* less than 0.05 was considered significant.

Reproducibility Assessment.—All hematoxylin and eosin-stained slides containing tumor from 23 randomly selected cases were scanned in an Aperio Scanner (Leica Biosystem). Whole slide images (WSIs) were reviewed by five observers by telepathology. The number of WSI per case ranged from one to five slides. Fleiss' κ statistic was used to measure the reliability of agreement among observers. Scoring agreement was evaluated as having either total or most agreement. Total agreement was defined as concordance between all observers at the three grades. Most agreement was defined as the exact scoring agreement in at least three of five observers. The strength of association (agreement) was categorized as follows: 1.00: perfect agreement; 0.80 to 0.99: almost perfect agreement; 0.60 to 0.79: substantial agreement; 0.40 to 0.59: moderate agreement; 0.20 to 0.39: fair agreement; 0.0 to 0.19: poor agreement; less than 0: no agreement.[35]

Results

Histologic Evaluation and Cinical Characteristics—Training Set

The distribution of predominant histologic patterns is illustrated in Table 1. There was a strong association of histologic features (nuclear, cytologic, mitotic grade, and STAS) with histologic patterns with hot-spot evaluation. High nuclear grade, higher number of mitotic figures, and the presence of STAS were seen in association with high-grade histologic patterns, whereas low- and intermediate-grade histologic patterns exhibited predominantly low- or intermediate-mitotic rate and nuclear grade ($p < 0.001$) (Supplementary Fig. 2). No STAS was recorded in tumors without a high-grade pattern component. Necrosis was recorded in 26 cases, all in high-grade predominant tumors.

Low-grade cytology was recorded predominantly in lepidic, acinar, papillary, and micropapillary histologic patterns (85% of the cases), whereas only 15% were recorded in solid and complex glandular patterns. Like-wise, high-grade cytology was seen predominantly in solid and complex glandular patterns (85% of the cases), whereas it was recorded in 14% of acinar, papillary, and micropapillary patterns, and 1% in lepidic pattern.

Building of the Grading Model—Role of Histologic Patterns

The association of histologic features with recurrence rates in the training cohort is illustrated in Supplementary Table 1.

The prognostic distinguishing ability of a model with patient characteristics only (age, sex, and clinical stage) was represented by an AUC of 0.685 for recurrence and 0.673 for death. In an attempt to improve the AUC curve, histologic features were added. These include adding the predominant pattern only, a combination of the two most predominant patterns, the predominant plus high-grade patterns, and the weighted average, binary, or numeric combinations of all patterns as variables to the model. The results are illustrated in Table 2. Introduction of the predominant pattern only to clinical characteristics improved the prognostic stratification of the model with an AUC of 0.719 for recurrence and 0.729 for death, but the greatest increment to the curve comes from the combination of the two most predominant patterns (AUC = 0.765 for RFS and AUC = 0.760 for OS) and the predominant plus high-grade patterns (AUC = 0.749 for RFS and AUC = 0.741 for OS).

Adding all patterns to the model either as weighted average or binary was equally predictive compared with the combination of the two most predominant or predominant plus high-grade model.

Because the difference in AUC for the two of the top performing models (two most predominant and predominant plus high-grade) was not statistically different, it was decided to concentrate on the latter, as it is more practical for pathologists who tend to grade on the basis of the worst differentiated pattern. All other possible combinations were not further evaluated.

Next, we evaluated the minimal percentage of high-grade (solid, micropapillary, and complex glandular) patterns required to influence the performance of the model. A cutoff

of less than 10% is not efficient (sensitivity 1, specificity 0), and a cutoff of 10% led to sensitivity of 0.47 and specificity of 0.76. A cutoff of 20% for high-grade patterns was the value that offered the best combination of sensitivity and specificity of the curve (0.64 and 0.68, respectively). The application of the 20% cutoff for high-grade patterns resulted in AUC of 0.749 for recurrence and 0.787 for death.

We next evaluated if other histologic features could improve the model. The effect of the various histologic features, either singly or in combination, was tested for their effects on AUC. None of the histologic features substantially improved the AUC of the new reference model (Table 3).

On the basis of the results, a new grading system (the IASLC grading system, Table 4), which includes the following, was proposed:

Grade 1: well-differentiated adenocarcinoma: lepidic predominant tumors with no or less than 20% of high-grade patterns (solid, micro papillary, and/or complex glandular patterns).

Grade 2: moderately differentiated adenocarcinomas: acinar or papillary predominant tumors with no or less than 20% of high-grade patterns.

Grade 3: poorly differentiated: any tumor with 20% or more of high-grade patterns.

Validation Set

Similar analysis was performed in the validation cohort in which the median time for recurrence was 1407 (range 778–1984) days and time to death was 1995 (range 1772–2225) days. All the following histologic parameters were associated with recurrence: predominant histologic patterns ($p = 0.05$), nuclear grade ($p = 0.01$), cytologic grade ($p = 0.0002$), mitotic grade ($p = 0.004$), and presence of STAS ($p = 0.03$) (Supplementary Table 2).

Similar to the training cohort, the combination of the predominant plus high-grade patterns (AUC = 0.732) was the best indicator of recurrence. Addition of any other histologic features either in combination or as single features did not reveal improvement of the model (Supplementary Table 3).

Test Cohort

The model was tested in a cohort of 300 stage I to III adenocarcinomas. In this cohort, the median time for recurrence was 570 (range 306–1200) days and time to death was 1195 (range 660–1998) days.

The model revealed a similar performance in the test cohort with AUC of 0.690 (range 0.629–0.751) and C-index of 0.704 for recurrence and AUC of 0.743 (range 0.688–0.797) and C-index of 0.729 for death (Supplementary Table 4).

The predictive performance of the IASLC final model (Table 4) was compared with the performance of a predominant pattern grading system in the test cohort. Higher grade was associated with reduced RFS with both grading systems, either in the entire cohort (stage I–III) or stage I cohort only; however, the stratification of survival between the 3 grades was

more evident with the IASLC grading system than the predominant pattern-based grading system ($p < 0.0001$ versus $p = 0.00013$ for the entire cohort (Fig. 2A and B) and $p = 0.0093$ versus $p = 0.044$ for stage I cohort) (Fig. 2C and D). Similar performance was seen with OS. Higher grade was associated with reduced OS with both grading systems in the entire and stage I cohorts ($p = 0.00011$ versus $p < 0.0001$ for the entire cohort and $p = 0.0053$ versus $p = 0.011$ for stage I cohort).

Reproducibility Assessment

Five observers reviewed WSI representing all slides from 23 cases. There was total agreement in 52% of cases (12 of 23) and major agreement in 47% (11 of 23) among observers leading to a k value of 0.617 (SE = 0.0478; 95% confidence interval: 0.5238–0.7095). Most of the disagreements were recorded between grades 1 and 2 (6 of 23, 26%) with some observers classifying an adenocarcinoma pattern as lepidic and others as papillary. Discordant results for grades 2 and 3 (5 of 23, 22%) were mostly owing to observed differences in the proportion of high-grade patterns. In summary, there was substantial agreement by Fleiss' κ test, and there was almost perfect agreement between pairs of the observers (Supplementary Table 5).

Discussion

Our results reveal that a grading system based on a histologic pattern is a strong prognostic classifier of invasive pulmonary adenocarcinoma. Given that it builds directly from the current classification system, it can be readily and reproducibly applied in practice. The proposed IASLC grading system considers the heterogeneity and relative proportion of architectural patterns within a tumor to arrive at a common language for prognostic groups, thus, paving the way for studies evaluating response and prognosis of pulmonary adenocarcinoma.

On the basis of the proposed grading system, any tumor with 20% or more of high-grade patterns should be classified as poorly differentiated because these tumors behave in a more aggressive fashion similar to those with predominant high-grade pattern. The proposed grading system offers a superior prognostic grouping compared with that of the predominant pattern only.

The strength of this study is the use of several independent data sets from different institutions, thus, reducing institutional and pathologists' biases. The model was created using one well-annotated data set, in which several possible alternatives were tested and then validated in another well-annotated data set, in which the same parameters evaluated in the training data set were tested and confirmed. The final model was finally tested on a third data set. The latter, different from the other data sets, was not reviewed specifically for the study but rather represented historical collections from contributing institutions. The fact that the model performed similarly in all data sets supports its robustness.

It is worth noting that the power of histologic characteristics of tumors as a tool for prognosis prediction is limited. In our studies, the best AUC was just over 0.7 in all data sets evaluated. Similar observation and results were also found in other publications.

For instance, Sica et al.[20] proposed a pattern-based grading system and found that the best estimate was 0.65 (95% confidence interval 0.57–0.73) using concordance probability estimate instead of AUC. Similarly, Liu et al.[30] proposed a model integrating T stage, histologic pattern, and necrosis which also obtained an AUC of 0.717. This suggests that there might be other nonhistologic characteristics of tumors that may increase the predictability of recurrence. Some investigators have proposed a molecular grading system on the basis of cell cycle gene expressions as a way to predict recurrence in stage I to II tumors[36–38]; however, no reference to a histologic evaluation is available in these studies. It is hoped that future studies may be able to incorporate the IASLC grading system in their investigations to identify other biomarkers that can improve prediction of recurrence of the disease or death.

It is interesting to note that other histologic features that have been reported to have prognostic significance in predicting recurrence in stage I adenocarcinomas did not add a value to the model proposed here. Our results reveal that most of the histologic features, such as nuclear and cytologic grades, STATS, and mitotic grade, are associated with histologic patterns either in the predominant or nonpredominant patterns. Although lymphatic invasion was not evaluated in this study, it has been reported that it is associated with high-grade patterns.[39,40] It is also important to note that the proposed grading system has not been validated in variants of adenocarcinoma, including invasive mucinous adenocarcinoma. Further studies are necessary to evaluate the applicability and performance of the model in these special tumors.

Another important determination from this study was the establishment of a cutoff for high-grade patterns, as many reports in the literature had provided conflicting percentages for high-grade patterns as determinant of recurrence. A cutoff of 20% offered the best sensitivity and specificity to the AUC in this study. It is interesting to note that Sica et al.[20] have also suggested that tumors with 20% solid or micropapillary pattern had already a significant metastatic potential, compared with other histologic patterns.

Reproducibility of histologic pattern assessments among multiple pathologists can be challenging.[41] In this study, we have reported almost perfect agreement on grading between two observers (a total of 10 pathologist pairs) evaluating 23 cases with kappa values ranging from 0.79 to 0.89 (the mean kappa value: 0.84 ± 0.04). Of note, most of the discrepant grades were attributed to the differentiation of lepidic versus papillary patterns (grade 1 versus grade 2) followed by the difference in the proportion of high-grade patterns. Thus, refinement of definitions of lepidic and invasive patterns will likely improve reproducibility.[42]

In summary, this study proposes a new grading system for invasive pulmonary adenocarcinoma. The grading model is practical and based on pattern recognition, which allows its quick implementation in routine pathology practice, as it does not require the pathologist to learn additional technologies. The model offers a new prognostic grouping for pulmonary adenocarcinoma that is reproducible in multiple data sets from different institutions. It is hoped that this grading system will provide a common language to be used by pathologists in clinical practice and investigators evaluating prognostic and

or predictive markers in adenocarcinoma and allow for more comprehensive comparison of the histologically heterogeneous tumors. Finally, this grading system is not meant to replace the current classification of pulmonary adenocarcinoma but is rather considered as a complement.

Supplementary Material

Refer to Web version on PubMed Central for supplementary material.

Acknowledgments

This project was supported by grants from the International Association for the Study of Lung Cancer and the National Institutes of Health/National Cancer Institute Early Detection Research Network 1U01CA214195–01 to HP used for biospecimen collection and salary support (DFL). The authors thank the staff of the Center of Biospecimen Research and Development from the New York University for their help in digital pathology and histology for this project. The Center of Biospecimen Research and Development is partially supported by the Cancer Center Support Grant P30CA016087 at the Laura and Isaac Perlmutter Cancer Center.

Disclosure: Dr. Beasley reports receiving personal fees from LOXO Oncology and various law firms, outside of the submitted work. Dr. Botling reports receiving personal fees from AstraZeneca, Merck Sharp & Dohme, Roche, Pfizer, Boehringer Ingelheim, Novartis, and Illumina; grants and personal fees from Bristol-Myers Squibb, outside of the submitted work. Dr. Bubendorf reports receiving grants and personal fees from Roche and Merck Sharp & Dohme; personal fees from Bristol-Myers Squibb, Takeda, Bayer, Eli Lilly, Pfizer, and Boehringer Ingelheim, outside of the submitted work. Dr. Dacic reports receiving personal fees from AstraZeneca, Bayer, Takeda, and Bristol-Myers Squibb, outside of the submitted work. Dr. Ferrari-Light reports receiving other compensation for data from Intuitive Surgical Inc., which is outside of and unrelated to the submitted work. Dr. Lopez-Rios reports receiving grants and personal fees from Thermo Fisher, Bristol-Myers Squibb, Roche, Eli Lilly, Pfizer, and Merck Sharp & Dohme; personal fees from AstraZeneca and Bayer, outside of the submitted work. Dr. Mino-Kenudson reports receiving personal fees from H3 Biomedicine and AstraZeneca; grants from Novartis, outside of the submitted work. Dr. Motoi reports receiving grants and personal fees from Roche Diagnostics and Ono Pharmaceutical; grants from NEC; personal fees from Bristol-Myers Squibb Japan, Agilent, Cook Japan, Merck Sharp & Dohme, Miraca Life Science, AstraZeneca, Novartis, Chugai, Taiho, Beckton Dickinson Japan, and Covidien Japan, outside of the submitted work. Dr. Nicholson reports receiving personal fees from Merck, Boehringer Ingelheim, Novartis, AstraZeneca, Bristol-Myers Squib, Roche, AbbVie, and Oncologica; grants and personal fees from Pfizer, outside of the submitted work. Dr. Papotti reports receiving personal fees from AstraZeneca, Roche, Pfizer, Merck Sharp & Dohme, AbbVie, and Eli Lilly, outside of the submitted work. Dr. Sholl reports receiving personal fees from LOXO Oncology, AstraZeneca, EMD Serono, and Foghorn Therapeutics; grants from Roche Genentech, outside of the submitted work. Dr. Wistuba reports receiving grants and personal fees from Genentech/Roche, Bayer, Bristol-Myers Squibb, AstraZeneca/Medimmune, Pfizer, HTG Molecular, Asuragen, Merck, and Guardant Health; personal fees from Merck Sharp & Dohme, GlaxoSmithKline, and Oncocyte; grants from Oncoplex, DepArray, Adaptive, Adaptimmune, EMD Serono, Takeda, Amgen, Karus, Johnson & Johnson, Iovance, 4D, Novartis, and Akoya, outside of the submitted work. Dr. Yatabe reports receiving personal fees from Chugai Pharmaceutical, Merck Sharp & Dohme, AstraZeneca, Pfizer, Novartis, Ventana-Roche, Dako-Agilent, and Thermo Fisher Scientific, outside of the submitted work. The remaining authors declare no conflict of interest.

References

1. Amin MB, Edge S, Greene F, et al., eds. AJCC Cancer Staging Manual. 8th ed.Chicago, IL: Springer International Publishing; 2017.
2. Rabe K, Snir OL, Bossuyt V, Harigopal M, Celli R, Reisenbichler ES. Interobserver variability in breast carcinoma grading results in prognostic stage differences. Hum Pathol2019;94:51–57. [PubMed: 31655171]
3. Helpap B, Ringli D, Tonhauser J, et al.The significance of accurate determination of Gleason score for therapeutic options and prognosis of prostate cancer. Pathol Oncol Res2016;22:349–356. [PubMed: 26563277]
4. Tolonen TT, Kujala PM, Tammela TL, Tuominen VJ, Isola JJ, Visakorpi T. Overall and worst Gleason scores are equally good predictors of prostate cancer progression. BMC Urol2011;11:21. [PubMed: 21978318]

5. Rice-Stitt T, Valencia-Guerrero A, Cornejo KM, Wu CL. Updates in histologic grading of urologic neoplasms. Arch Pathol Lab Med2020;144:335–343. [PubMed: 32101058]
6. Travis WD, World Health Organization, International Agency for Research on Cancer, International Association for the Study of Lung Cancer, International Academy of Pathology. WHO Classification of Tumours of the Lung, Pleura, Thymus and Heart. Lyon and Oxford: IARC Press, Oxford University Press (distributor); 2015.
7. Tsao MS, Marguet S, Le Teuff G, et al.Subtype classification of lung adenocarcinoma predicts benefit from adjuvant chemotherapy in patients undergoing complete resection. J Clin Oncol2015;33:3439–3446. [PubMed: 25918286]
8. Yoshizawa A, Motoi N, Riely GJ, et al.Impact of proposed IASLC/ATS/ERS classification of lung adenocarcinoma: prognostic subgroups and implications for further revision of staging based on analysis of 514 stage I cases. Mod Pathol2011;24:653–664. [PubMed: 21252858]
9. Yoshizawa A, Sumiyoshi S, Sonobe M, et al.Validation of the IASLC/ATS/ERS lung adenocarcinoma classification for prognosis and association with EGFR and KRAS gene mutations: analysis of 440 Japanese patients. J Thorac Oncol2013;8:52–61. [PubMed: 23242438]
10. Woo T, Okudela K, Mitsui H, et al.Prognostic value of the IASLC/ATS/ERS classification of lung adenocarcinoma in stage I disease of Japanese cases. Pathol Int2012;62:785–791. [PubMed: 23252867]
11. Warth A, Muley T, Kossakowski C, et al.Prognostic impact and clinicopathological correlations of the cribriform pattern in pulmonary adenocarcinoma. J Thorac Oncol2015;10:638–644. [PubMed: 25634008]
12. Warth A, Muley T, Meister M, et al.The novel histologic International Association for the Study of Lung Cancer/American Thoracic Society/European Respiratory Society classification system of lung adenocarcinoma is a stage-independent predictor of survival. J Clin Oncol2012;30:1438–1446. [PubMed: 22393100]
13. Branca G, Ieni A, Barresi V, Tuccari G, Caruso RA. An updated review of cribriform carcinomas with emphasis on histopathological diagnosis and prognostic significance. Oncol Rev2017;11:317. [PubMed: 28382188]
14. Xu L, Tavora F, Burke A. Histologic features associated with metastatic potential in invasive adenocarcinomas of the lung. Am J Surg Pathol2013;37:1100–1108. [PubMed: 23681071]
15. Makinen JM, Laitakari K, Johnson S, et al.Histological features of malignancy correlate with growth patterns and patient outcome in lung adenocarcinoma. Histopathology. 2017;71:425–436. [PubMed: 28401582]
16. Moreira AL, Joubert P, Downey RJ, Rekhtman N. Cribriform and fused glands are patterns of high-grade pulmonary adenocarcinoma. Hum Pathol2014;45:213–220. [PubMed: 24439219]
17. Kuang M, Shen X, Yuan C, et al.Clinical significance of complex glandular patterns in lung adenocarcinoma: clinicopathologic and molecular study in a large series of cases. Am J Clin Pathol2018;150:65–73. [PubMed: 29746612]
18. Kadota K, Yeh YC, Sima CS, et al.The cribriform pattern identifies a subset of acinar predominant tumors with poor prognosis in patients with stage I lung adenocarcinoma: a conceptual proposal to classify cribriform predominant tumors as a distinct histologic subtype. Mod Pathol2014;27:690–700. [PubMed: 24186133]
19. Kadota K, Kushida Y, Kagawa S, et al.Cribriform subtype is an independent predictor of recurrence and survival after adjustment for the eighth edition of TNM staging system in patients with resected lung adenocarcinoma. J Thorac Oncol2019;14:245–254. [PubMed: 30336325]
20. Sica G, Yoshizawa A, Sima CS, et al.A grading system of lung adenocarcinomas based on histologic pattern is predictive of disease recurrence in stage I tumors. Am J Surg Pathol2010;34:1155–1162. [PubMed: 20551825]
21. Nakazato Y, Minami Y, Kobayashi H, et al.Nuclear grading of primary pulmonary adenocarcinomas: correlation between nuclear size and prognosis. Cancer. 2010;116:2011–2019. [PubMed: 20151423]
22. von der Thusen JH, Tham YS, Pattenden H, et al.Prognostic significance of predominant histologic pattern and nuclear grade in resected adenocarcinoma of the lung: potential parameters for a grading system. J Thorac Oncol2013;8:37–44. [PubMed: 23242436]

23. Kadota K, Suzuki K, Kachala SS, et al.A grading system combining architectural features and mitotic count predicts recurrence in stage I lung adenocarcinoma. Mod Pathol2012;25:1117–1127. [PubMed: 22499226]
24. Duhig EE, Dettrick A, Godbolt DB, et al.Mitosis trumps T stage and proposed international association for the study of lung cancer/American Thoracic Society/European Respiratory Society classification for prognostic value in resected stage 1 lung adenocarcinoma. J Thorac Oncol2015;10:673–681. [PubMed: 25514800]
25. Kadota K, Nitadori J, Sima CS, et al.Tumor spread through air spaces is an important pattern of invasion and impacts the frequency and location of recurrences after limited resection for small stage I lung adenocarcinomas. J Thorac Oncol2015;10:806–814. [PubMed: 25629637]
26. Warth A. Spread through air spaces (STAS): a comprehensive update. Transl Lung Cancer Res2017;6:501–507. [PubMed: 29114466]
27. Shih AR, Mino-Kenudson M. Updates on spread through air spaces (STAS) in lung cancer [e-pub ahead of print]. Histopathology. 10.1111/his.14062.Accessed June 29, 2020.
28. Toyokawa G, Yamada Y, Tagawa T, Oda Y. Significance of spread through air spaces in early-stage lung adenocarcinomas undergoing limited resection. Thorac Cancer. 2018;9:1255–1261. [PubMed: 30079987]
29. Masai K, Sakurai H, Sukeda A, et al.Prognostic impact of margin distance and tumor spread through air spaces in limited resection for primary lung cancer. J Thorac Oncol2017;12:1788–1797. [PubMed: 28882585]
30. Liu DH, Ye ZH, Chen S, et al.Novel prognostic model for stratifying survival in stage I lung adenocarcinoma patients. J Cancer Res Clin Oncol2020;146:801–807. [PubMed: 31884561]
31. Bains S, Eguchi T, Warth A, et al.Procedure-specific risk prediction for recurrence in patients undergoing lobectomy or sublobar resection for small (≤2 cm) lung adenocarcinoma: an international cohort analysis. J Thorac Oncol2019;14:72–86. [PubMed: 30253972]
32. Nitadori J, Bograd AJ, Kadota K, et al.Impact of micropapillary histologic subtype in selecting limited resection vs lobectomy for lung adenocarcinoma of 2cm or smaller. J Natl Cancer Inst2013;105:1212–1220. [PubMed: 23926067]
33. Kadota K, Villena-Vargas J, Yoshizawa A, et al.Prognostic significance of adenocarcinoma in situ, minimally invasive adenocarcinoma, and nonmucinous lepidic predominant invasive adenocarcinoma of the lung in patients with stage I disease. Am J Surg Pathol2014;38:448–460. [PubMed: 24472852]
34. Emoto K, Eguchi T, Tan KS, et al.Expansion of the concept of micropapillary adenocarcinoma to include a newly recognized filigree pattern as well as the classical pattern based on 1468 stage I lung adenocarcinomas. J Thorac Oncol2019;14:1948–1961. [PubMed: 31352072]
35. Viera AJ, Garrett JM. Understanding interobserver agreement: the kappa statistic. Fam Med2005;37:360–363. [PubMed: 15883903]
36. Rakha E, Pajares MJ, Ilie M, et al.Stratification of resectable lung adenocarcinoma by molecular and pathological risk estimators. Eur J Cancer. 2015;51:1897–1903. [PubMed: 26235745]
37. Aramini B, Casali C, Stefani A, et al.Prediction of distant recurrence in resected stage I and II lung adenocarcinoma. Lung Cancer. 2016;101:82–87. [PubMed: 27794412]
38. Eguchi T, Kadota K, Chaft J, et al.Cell cycle progression score is a marker for five-year lung cancer-specific mortality risk in patients with resected stage I lung adenocarcinoma. Oncotarget. 2016;7:35241–35256. [PubMed: 27153551]
39. Chang C, Sun X, Zhao W, et al.Minor components of micropapillary and solid subtypes in lung invasive adenocarcinoma (≤3 cm): PET/CT findings and correlations with lymph node metastasis. Radiol Med2020;125:257–264. [PubMed: 31823295]
40. Kosaka T, Shimizu K, Nakazawa S, et al.Clinicopathological features of small-sized peripheral squamous cell lung cancer. Mol Clin Oncol2020;12:69–74. [PubMed: 31814978]
41. Thunnissen E, Beasley MB, Borczuk AC, et al.Reproducibility of histopathological subtypes and invasion in pulmonary adenocarcinoma. An international interobserver study. Mod Pathol2012;25:1574–1583. [PubMed: 22814311]

42. Shih AR, Uruga H, Bozkurtlar E, et al.Problems in the reproducibility of classification of small lung adenocarcinoma: an international interobserver study. Histopathology. 2019;75:649–659. [PubMed: 31107973]

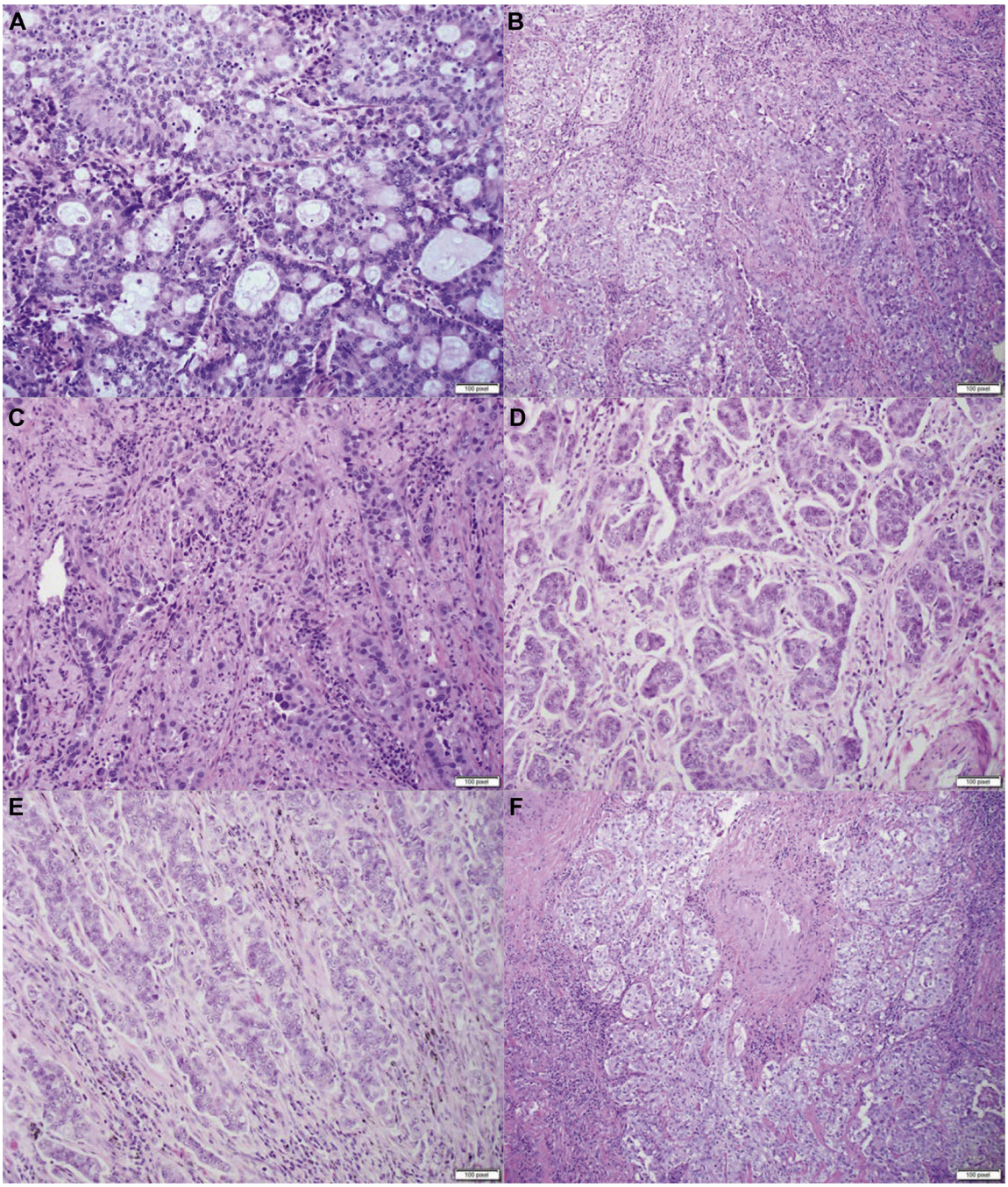

Figure 1.

Histologic examples of complex glandular patterns. (*A*) Cribriform pattern characterized by nests of neoplastic cells with sieve-like perforations; (*B*) poorly formed glands in a continuous spectrum between solid and acinar patterns; (*C*) fused and irregular glands in desmoplastic stroma; (*D–F*) poorly formed glands in a ribbon-like formation with irregular borders, small cell clusters, and single cells infiltrating desmoplastic stroma.

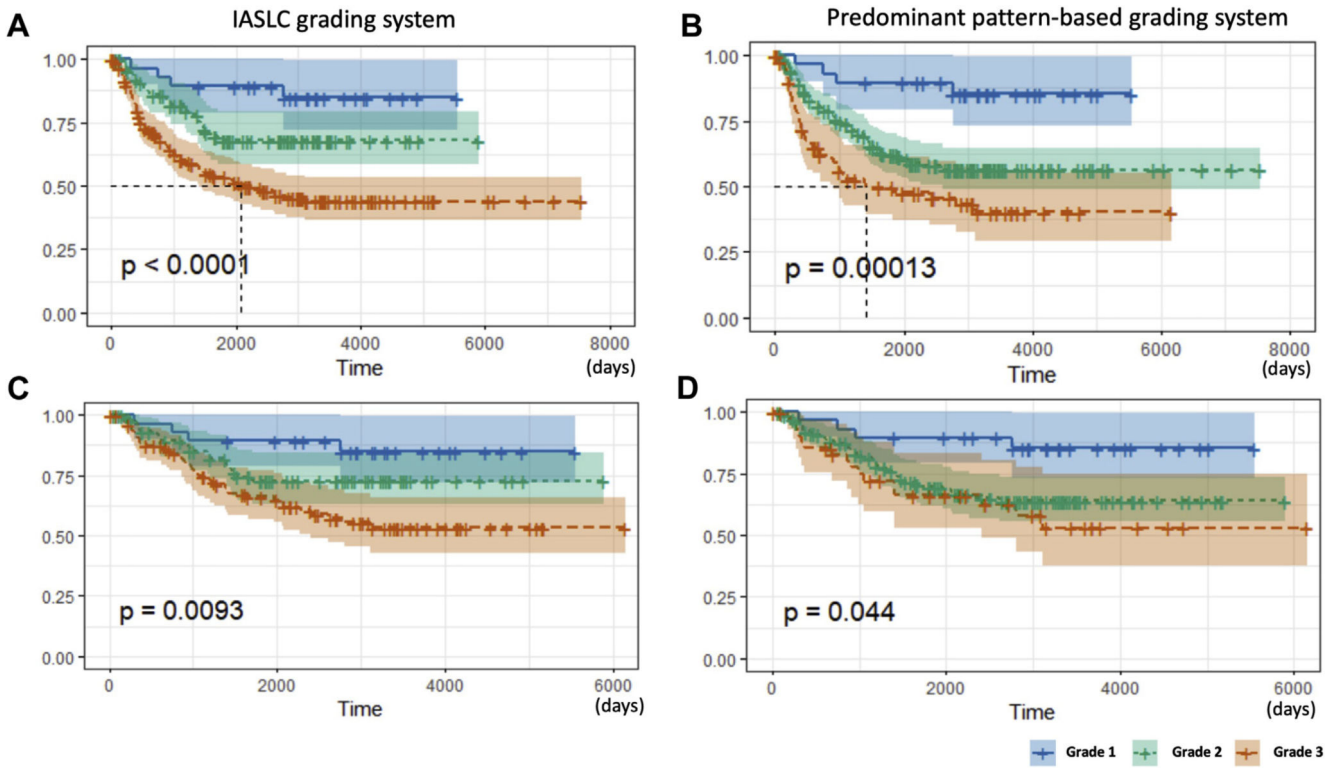

Figure 2.

Kaplan-Meier curves for RFS of the test cohort stratified by the IASLC grading system (*A*: the entire cohort and *C*: stage I cohort) and predominant pattern-based grading system (*B*: the entire cohort and *D*: stage I cohort). For the latter, grade 1 is composed of lepidic predominant tumors; grade 2 of acinar and papillary predominant tumors, and grade 3 of solid, micropapillary, and complex glandular predominant tumors. IASLC, International Association for the Study of Lung Cancer; RFS, recurrence-free survival.

Table 1.

Patients' Demographic Information on All Cohorts

Characteristics	Training Cohort (n = 284)	Validation Cohort (n = 212)	Test Cohort (n = 300)
Age, mean ± SD	69.2 ± 8.9	69 ± 9.2	66 ± 10.9
Sex, n (%)			
Male	90 (32)	140 (66)	141 (47)
Female	194 (68)	72 (34)	159 (53)
Race, n (%)			
White	247 (87)	191 (90)	–
Asian	23 (8)	10 (4.7)	–
Black	4 (1)	6 (2.8)	–
Hispanic	8 (3)	4 (2)	–
Other/unknown	2 (1)	1 (0.5)	300 (100)
Type of operation, n (%)			
Lobectomy	179 (63)	122 (58)	231 (77)
Segmentectomy	66 (23)	16 (8)	12 (4)
Wedge	39 (14)	74 (35)	47 (16)
Pneumonectomy	0	0	10 (3)
Pathologic stage, n (%)			
IA	229 (81)	107 (50.5)	132 (44)
IB	55 (19)	105 (49.5)	74 (25)
IIA	0	0	12 (4)
IIB	0	0	43 (14)
IIIA	0	0	32 (11)
IIIB	0	0	7 (2)
Alive status, n (%)			
Alive	248 (87)	188 (89)	140 (47)
Dead	36 (13)	24 (11)	160 (53)
Predominant histologic pattern, n (%)			
Acinar	129 (45)	77 (36)	131 (43)
Papillary	55 (19)	24 (11)	47 (15)

Characteristics	Training Cohort (n = 284)	Validation Cohort (n = 212)	Test Cohort (n = 300)
Lepidic	20 (7)	67 (32)	30 (10)
Solid	40 (14)	21 (10)	67 (22)
Micropapillary	21 (7)	13 (6)	16 (7)
Complex glands (cribriform and fused glands)	19 (7)	10 (5)	9 (3)

Table 2.

Selection of Variables for Histologic Patterns in the Training Set

	Recurrence		Death	
Variables in the Model	**C-Index**	**AUC**	**C-Index**	**AUC**
Baseline	0.65	0.68	0.68	0.673
Baseline + predominant pattern	0.698	0.719	0.727	0.729
Baseline + predominant pattern + secondary pattern	0.742	0.765	0.764	0.760
Baseline + predominant pattern + high-grade pattern	0.740	0.749	0.758	0.741
Baseline + predominant pattern + high-grade pattern (20% cutoff)	0.732	0.749	0.732	0.787
Baseline + weighted average	0.698	0.719	0.742	0.733
Baseline + pattern 1 + pattern 2 + pattern 3 (binary)[a]	0.726	0.734	0.732	0.714
Baseline + pattern 1 + pattern 2 + pattern 3 (numeric)[a]	0.733	0.742	0.746	0.735
Baseline + all 7 patterns (binary)[a]	0.744	0.756	0.754	0.757
Baseline + all 7 patterns (numeric)[a]	0.745	0.755	0.759	0.747

Baseline model represent clinical characteristics only.

[a]Patterns 1 to 3 indicate the following three-tiered classification of predominant pattern in the tumor: pattern 1, lepidic; pattern 2, acinar or papillary; pattern 3, micropapillary, solid, or complex glandular pattern (cribriform and fused glands). All seven patterns indicate that all patterns present in the tumor are individually counted. Binary represents presence or absence of patterns but assigned a number (1–3) as described previously. Numeric indicates that the numerical proportion of that pattern was taken into consideration.

AUC, area under the ROC curve; C-index, concordance index; ROC, receiver operating characteristic.

Table 3.

Selection of Histologic Features in the Model of Predominant Plus High-Grade Patterns (With a Cutoff of 20% or More for High-Grade Patterns)

	Recurrence		Death	
Variables in the Model	**C-Index**	**AUC**	**C-Index**	**AUC**
Baseline + predominant + high-grade patterns (20% cutoff)	0.739	0.749	0.732	0.787
Mitotic grade + nuclear grade + cytologic grade + STAS[a]	0.741	0.746	0.775	0.761
Mitotic grade + cytologic grade + STAS[a]	0.743	0.748	0.787	0.769
Cytologic grade + STAS[a]	0.741	0.752	0.785	0.768
STAS[a]	0.740	0.752	0.785	0.765

[a]Training set: adding the histologic features to baseline + predominant plus high-grade patterns (backward selection, remove the least significant variable each time). Addition of other histologic features (nuclear grade, mitotic grade, STAS, etc.) did not improve the model.

AUC, area under the ROC curve; C-index, concordance index; ROC, receiver operating characteristic; STAS, spread through airspace.

Table 4.

Grading Scheme for Invasive Pulmonary Adenocarcinomas

Grade	Differentiation	Patterns
1	Well-differentiated	Lepidic predominant with no or less than 20% of high-grade patterns
2	Moderately differentiated	Acinar or papillary predominant with no or less than 20% of high-grade patterns
3	Poorly differentiated	Any tumor with 20% or more of high-grade patterns

The model is based on the predominant histologic plus high-grade patterns. The latter includes solid, micropapillary, and complex glandular patterns.

J Thorac Oncol. Author manuscript; available in PMC 2021 August 13.